

Experimental and analytical study on flexural behaviour of fly ash and paper sludge ash based geopolymer concrete

P. Senthamilselvi*¹ and T. Palanisamy²

¹Department of Civil Engineering, Government College of Engineering, Salem 636 011, Tamil Nadu, India

²Department of Civil Engineering, KSR College of Engineering, Tiruchengode 637 215, Tamil Nadu, India

(Received July 11, 2017, Revised September 10, 2017, Accepted September 11, 2017)

Abstract. This article presents the flexural behaviour of reinforced fly ash (FA)-based geopolymer concrete (GPC) beams with partial replacement of FA for about 10% by weight with paper sludge ash (PSA). The beams were made of M35 grade concrete and cured under three curing conditions for comparison viz., ambient curing, external exposure curing, and oven curing at 60°C. The beams were experimentally tested at the 28th day of casting after curing by conducting two-point loading flexural test. Performance aspects such as load carrying capacity, first crack load, load-deflection and moment-curvature behaviours of both types of beams were experimentally studied and their results were compared under different curing conditions. To verify the response of reinforced GPC beams numerically, an ANSYS 13.0 finite element program was also used. The result shows that there is a good agreement between computer model failure behaviour with the experimental failure behaviour.

Keywords: geopolymer concrete; paper sludge ash; load deflection; curing; ANSYS

1. Introduction

The environmental issues associated with the production of ordinary Portland cement (OPC) are well known (Hardjito and Rangan 2005). One tonne of carbon dioxide gets released is for every tonne of OPC produced, because of calcination of limestone and combustion of fossil fuel during the manufacturing process. Over the past 20 years, a family of new materials called geopolymer also known as mineral or inorganic polymer glass, received attention as a promising new form of inorganic polymer material that could replace OPC, plastics and many mineral based products. However, currently, the precise mechanisms governing geopolymerization are still not fully understood (Hardjito and Rangan 2005). A geopolymeric reaction is a geosynthetic reaction of aluminosilicate minerals in the presence of an alkali solution. The reaction depends on the ability of the aluminium ion (sixfold or fourfold coordination) to induce crystallographical and chemical changes in a silica backbone under alkali activation (Davidovits 2005).

Materials rich in silicon (Si), such as fly ash (FA) or slag, and aluminium (Al), such as kaolin clay, are the primary requirement for geopolymerization (Khale and Chaudhary 2007).

Geopolymerization involves a heterogeneous chemical reaction between solid aluminosilicate oxides and alkali metal silicate solutions at highly alkaline condition and mild temperatures yielding amorphous to semi crystalline polymeric structure, which consists of Si-O-Al and Si-O-Si

bonds (Davidovits 1994). For geopolymerization technology, source materials rich in Si and Al, should be in amorphous form to undergo the alkaline activation process (Hardjito *et al.* 2004). The similarity of some fly ashes, due to the presence of silica (SiO₂) and alumina (Al₂O₃), has brightened the chances of using geopolymerization as a possible technology solution in preparing special cement (Silverstrim *et al.* 1997, 1999). At ambient temperature, the geopolymerization reaction rate of the raw FA is extremely low (Puertas *et al.* 2000). Temuujin *et al.* (2009) obtained increased compressive strength for geopolymer with mechanically activated FA cured at ambient temperature. The compressive strength of ambient-cured FA-GGBS based geopolymer mortar increases with an increase in ground-granulated blast furnace slag (GGBS) content and molarity of alkaline solution (Manjunath *et al.* 2011). The minimum compressive strength of concrete required for construction can also be achieved even at room temperature by using alccofine as a replacement material to fly ash in geopolymer concrete (Jindal *et al.* 2017, Parveen *et al.* 2017).

Paper sludge ash (PSA) is an another pozzolanic material that has not been extensively used in geopolymer application. It is generated from the incineration process of paper sludge, which is the largest by-product of the paper and pulp industry and is a major concern for the industry in terms of solid waste management (Geng *et al.* 2006, Battaglia *et al.* 2003). With incineration, the sludge can be converted into a pozzolanic product that is usable in the cement and concrete industries. The PSA comprises approximately 70-80% amorphous silica and alumina (Mun and Ahn 2001). Waste PSA and alkaline liquids were used to produce geopolymer concrete (GPC) by Ridzuan *et al.* (2013). In their work, the authors concluded that the compressive strength of partial PSA-based GPC incorporated

*Corresponding author, Professor
E-mail: senitaarul2004@yahoo.co.in

Table 1 Chemical composition of the fly ash and paper sludge ash (mass %)

Composition	SiO ₂	Al ₂ O ₃	Fe ₂ O ₃	CaO	MgO	Na ₂ O	SO ₃	K ₂ O	TiO ₂	LOI
Fly ash	53.97	34.66	5.3	1.96	1.28	0.13	0.25	0.93	1.52	2.6
Paper sludge ash	35.25	7.09	2.83	37.42	14.39	0.81	0.69	0.85	0.67	0.63

with recycled concrete aggregates increases with an increase in the molarity of sodium hydroxide. In this research work, PSA was used as a partial replacement material for FA to produce the GPC under three curing conditions.

Only a few studies are available on flexural behaviour of GPC beams. For replacement materials, the structural performance studies are limited. In the flexural strength studies on reinforced GPC beams, Wallah and Rangan (2006) reported that the behaviour and failure pattern of GPC beams were similar to those observed in the case of a reinforced Portland cement concrete (PCC) beam. Both experimental and analytical investigations on the shear behaviour of reinforced PCC and GPC beams were carried out and found that their behaviours are similar, but depends upon the FA content in GPC beams (Ambily *et al.* 2011).

To determine the flexural behaviour of reinforced GPC beams, both numerical studies using ABAQUS tool and experimental studies were carried out by Nguyen *et al.* (2016). The authors found that the flexural behaviour is good agreement in the finite element simulation using ABAQUS but its behaviour is quite different from the results provided by elastic theory designed for OPC. In the shear behaviour study of thin-walled *T*-beams, Madheswaran *et al.* (2014) established that the performance of reinforced GPC is similar to that of reinforced PCC beam and the loads are of the same order. Kannapiran *et al.* (2013) conducted a comparative study and concluded that the reinforced GPC shows high ultimate moment resistance compared to reinforced cement concrete beam. Dattatreya *et al.* (2011) conducted an experimental study on the flexural behaviour of room temperature cured reinforced GPC containing FA and GGBS and showed that conventional RC theory could be used for designing reinforced GPC beams. On conducting flexural behaviour test, Anuradha *et al.* (2012) found that GPC made with sand and manufactured sand had better structural integrity. Pires *et al.* (2014) investigated the fracture properties of reinforced GPC precast beams in which main precursors used were FA and rice husk ash. Their study results demonstrated that the reinforced GPC beams possess 20% higher toughness than OPC beams.

In this study, we investigated and compared the flexural behaviour of reinforced FA-GPC beams and reinforced FA-PSA GPC beams of M35 grade after 28 days of casting, for three different curing regimes namely, oven curing (OC), external exposure curing (EEC), and ambient curing (AC). The experimental results were verified numerically by using a finite element analysis (FEA) tool, ANSYS, version 13.0.

2. Materials

2.1 Fly ash

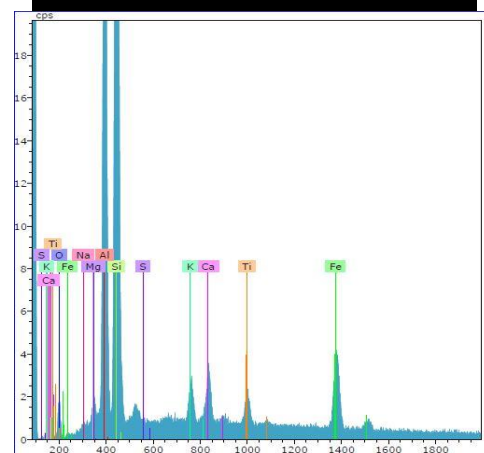
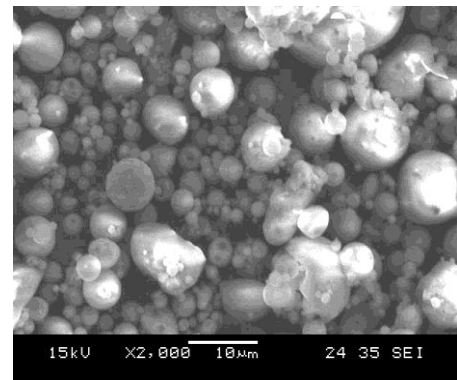


Fig. 1 SEM and EDX images of fly ash

In this investigation, class *F* fly ash, obtained from Mettur Thermal Power Station, Tamil Nadu, India was used as primary source material. The specific gravity of the FA was 2.29. The chemical properties of the FA was shown in Table 1. The scanning electron microscope (SEM) and energy-dispersive X-ray analysis (EDX) images of the FA are shown in Fig. 1. FA consists of spherical particles of different sizes.

2.2 Paper sludge ash

Paper sludge ash was obtained by incinerating separately the paper sludge obtained from Seshasayee Paper Mill (Pallipalayam, Erode, Tamil Nadu, India) at 700°C for 2 h. The specific gravity of the PSA was 2.3. The chemical property of the PSA was shown in Table 1. The SEM and EDX images of the PSA are shown Fig. 2. It can be seen that the PSA particles are dominantly hexagonal, platy, and less bulky.

2.3 Fine aggregate

River sand conforming to grading zone II as per BIS 383-1970 was used as a fine aggregate. Its specific gravity was 2.6 and fineness modulus was 2.72.

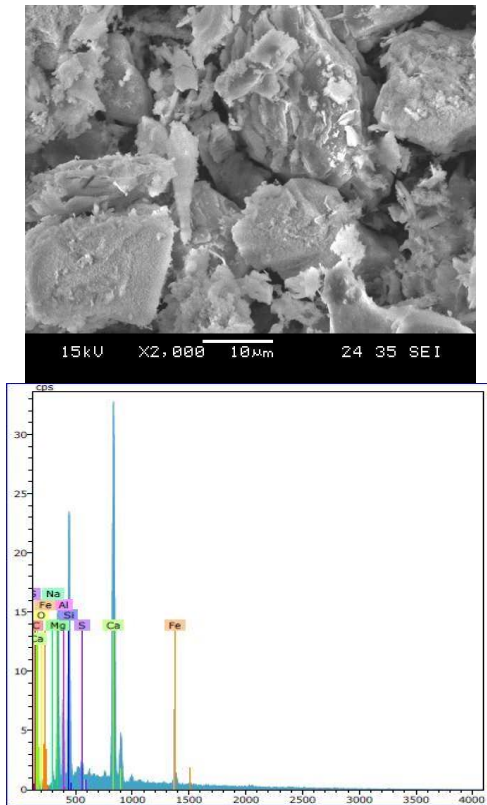


Fig. 2 SEM and EDX images of paper sludge ash

Table 2 Physical and chemical properties of sodium hydroxide

Appearance	Liquid (gel)
Colour	Light yellow liquid (gel)
Boiling point	100°C
Molecular weight	122.0632 g/mol
Specific gravity	1.53
Assay Na ₂ O	8.5%
Assay SiO ₂	28%
H ₂ O	63.5%

2.4 Coarse aggregate

Crushed blue granite stones of maximum 20 mm size were used as a coarse aggregate. The specific gravity of coarse aggregate was 2.86 and fineness modulus was approximately 7.27.

2.5 Alkaline activators

A mixture of sodium silicate and sodium hydroxide solutions was used as the alkaline liquid activator. Sodium hydroxide solution of 12 M was prepared by dissolving NaOH pellets of 99% purity in water. The ratio of sodium silicate to sodium hydroxide solutions by weight was kept as 2.5. The properties of NaOH and Na₂SiO₃ are shown in Tables 2 and 3, respectively.

3. Specimen details

Table 3 Physical and chemical properties of sodium silicate

Appearance	White crystalline substance
Colour	White
Molecular weight	39.997 g/mol
Specific gravity	1.52
Assay	99%
Carbonate (Na ₂ CO ₃)	1%
Chloride (Cl)	0.01%
Sulphate (SO ₂)	0.01%
Lead (Pb)	0.002%
Iron (Fe)	0.002%
Aluminium	0.002%

Table 4 Mix proportion (kg/m³)

Mix code	Fly ash	PSA	Coarse aggregate	Fine aggregate	NaOH solution	Na ₂ SiO ₃ solution	Curing condition
FA-GPC	425.73	0.00	1212.60	642.50	54.74	136.84	Oven
OC							
FA-PSA GPC	383.16	42.57	1212.60	642.50	54.74	136.84	External exposure
OC							
FA-GPC	425.73	0.00	1212.60	642.50	54.74	136.84	Ambient temperature
EEC							
FA-PSA GPC	383.16	42.57	1212.60	642.50	54.74	136.84	Ambient temperature
AC							

Twelve reinforced GPC beams were casted, among which six were of FA-GPC beams and the remaining were FA-PSA GPC beams. The grade of concrete was M35, and all the rods used for reinforcement were high yield strength deformed (HYSD) bars of Fe 500 grade were used for reinforcement. The detailed mix proportions for manufacturing GPC as per guidelines given in IS 10262-2009 are shown in Table 4. All the beams were designed for an under-reinforced section with the size of 125×250×2000 mm using two 12-mm diameter HYSD bars at the bottom and two 10-mm HYSD bars at the top as reinforcement. Two-legged stirrups of 8-mm diameter bars at a spacing of 150 mm c/c were provided as shear reinforcement along the span of the beam. Each beam was designated using FA-GPC and FA-PSA GPC for 100% FA-based GPC and for optimum mix of 90% FA and 10% PSA-based GPC. The reinforcement details of the beam are shown in Fig. 3.

4. Manufacture of M35 grade geopolymer concrete beams

Sodium hydroxide in pellet form was weighed to suit 12

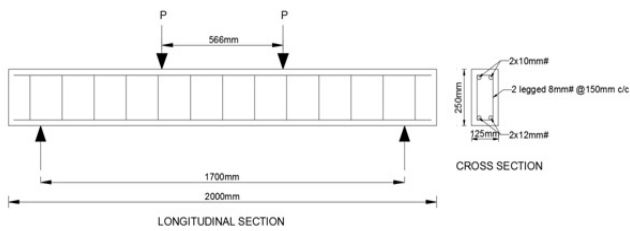


Fig. 3 Reinforcement details of the beam

M and dissolved in water. The solution was well-stirred for better dissolution and added to sodium silicate solution. Both solutions were mixed and kept in a container for 24 h before use. Dry materials were mixed in a pan mixer for 3-4 min and then the alkaline solution was added and allowed to get mixed for 4-5 min in order to make a uniform mix of concrete. Cover blocks were placed inside the mould before the placement of steel reinforcement. The steel reinforcement cage was placed above the cover blocks kept inside the steel mould and fresh concrete was poured in layers and was vibrated on a table vibrator for better compaction. As per the code IS 516-1959, the compressive strength was tested for the companion specimens using 150×150×150 mm mould.

5. Curing of geopolymer concrete beams

In this study, three curing regimes were used to observe the effect of temperature on the flexural behaviour of FA-GPC with and without PSA. The GPC specimens were exposed to three curing conditions: hot-air OC at 60°C, EEC, and AC. In the AC, the concrete specimens were placed in a shaded area with a maximum temperature of 28°C. These specimens were constantly protected from direct sunlight and rainfall until the testing. Meanwhile, in EEC the concrete specimens were placed in a non-protected area, exposed to direct sunlight yet protected from rainfall. The maximum temperature in externally exposed method reached to 41°C. For comparison, OC at 60°C exposure condition was also carried out for the specimens. Freshly cast specimens were given 1-day delay time before they were placed into the oven. After demoulding, the specimens were placed in an electrical oven at 60°C for 24 h. Then, the samples were shifted to ambient condition.

6. Test setup and instrumentation

The flexural test setup is shown in Fig. 4. All specimens were white-painted to facilitate crack marking. The capacity of the testing frame was approximately 1000 kN. The beams were simply supported over a span of 1700 mm and subjected to symmetrical two-point loads placed symmetrically over the span with about 566 mm distance between the loads. Dial gauges of 0.001 mm least count were used for measuring the deflections under the load points and at mid span. The dial gauge readings were recorded at different load intervals. Through visual observation, first crack loads (FCL) values were recorded.



Fig. 4 Experimental setup

Table 5 Compressive strength values of GPC.

Specimen ID	FA-GPC OC	FA-GPC EEC	FA-GPC AC	FA-PSA GPC OC	FA-PSA GPC EEC	FA-PSA GPC AC
Compressive strength (N/mm ²)	53	32	17	40	39	38

7. Test results and discussion

7.1 Compressive strength

The compressive strength values of GPC specimens, which were obtained as per Indian standards, are shown in Table 5.

The improvement in the compressive strength of FA-PSA-based GPC was 21.88% and 123.53% higher than that of the non-PSA-based specimens under EEC and AC conditions, respectively. But under OC condition, the inclusion of PSA adversely affected the strength performance of FA-based GPC. Because of PSA, the calcium compounds in the geopolymer mix improved the mechanical strength of the samples cured at ambient temperature but reduced the strength of the samples cured at higher temperature. The increase in the compressive strength of GPC with PSA at AC condition may be due to the pozzolanic reaction, which gets more pronounced at low temperature than at elevated temperature when PSA containing calcium compounds was used. The same was observed by Fernández *et al.* (2015) in their study, they found that the solubility of Al and Si increases significantly with the increase in temperature but it is not so with Ca compounds. This may be due to the possibility of the existence of different hardening mechanisms Shi *et al* (2006).

However, at day 28, it was observed that the PSA-added GPC did exceed the characteristic strength of 35 MPa and did attain the substantial strength of approximately 38 MPa for the 10% addition under EEC and AC conditions. Beyond 10% replacement of FA by PSA there is reduction in compressive strength of FA-PSA GPC under EEC and AC conditions.

7.2 Load carrying capacity

The specimens were tested by monotonically increasing the load until failure. Flexural cracks were developed with

Table 6 Experimental test result of beam

Beam ID	First crack load (kN)	Service load (kN)	Yield load (kN)	Ultimate load (kN)	Ultimate mid span deflection (mm)
FA-GPC OC	28.56	61.88	80	92.82	19.34
FA-GPC EEC	17.85	45.22	60	67.83	13.32
FA-GPC AC	7.14	33.32	42	49.98	10.84
FA-PSA GPC OC	24.99	59.5	78	89.25	15.2
FA-PSA GPC EEC	21.42	57.12	74	85.68	14.2
FA-PSA GPC AC	21.42	54.74	68	82.11	13.32

Table 7 Correlation of experimental and predicted ultimate moment of beams

Beam ID	Experimental ultimate moment (kN m)	Predicted ultimate moment (kN m)	Ratio of ultimate moment (experimental/predicted)
FA-GPC OC	26.299	20.603	1.276
FA-GPC EEC	19.21	19.702	0.975
FA-GPC AC	14.161	17.419	0.812
FA-PSA GPC OC	25.28	20.1126	1.256
FA-PSA GPC EEC	24.276	20.048	1.210
FA-PSA GPC AC	23.2645	19.993	1.163

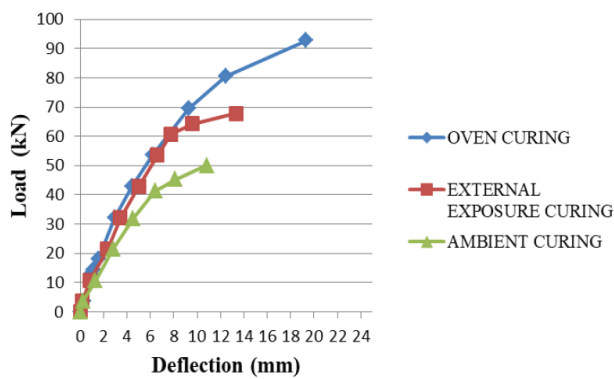


Fig. 5 Load vs mid span deflection curves of FA-GPC beams

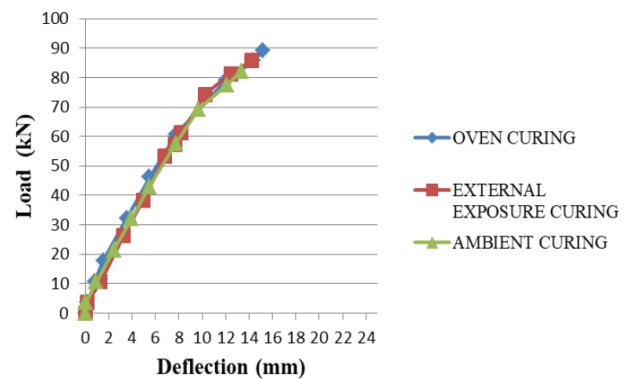


Fig. 6 Load vs mid span deflection curves of FA-PSA GPC beams

the increase of the load throughout the span of the beam. The progressive increase of deflection at mid span is shown as a function of increasing load. All beams behaved in a similar manner as they were designed as under-reinforced beams; that is, the tensile steel must have reached its yield strength before the concrete reaches its maximum capacity. The load carrying capacity (LCC) of the reinforced GPC beams at different stages is given in Table 6. Figs. 5 and 6 show the load deflection behaviour at mid span for the reinforced GPCspecimens.

7.3 Crack pattern and failure mode

Flexural cracks got initiated in the pure bending zone of beam on the tension side. They propagated as the load increased and new cracks started developed throughout the span.

Nearer to maximum load, the beams deflected significantly, indicating that the tensile steel must have yielded at failure.

The failure modes of all the beams are typical of the failure mode of an under reinforced concrete beam. The failure of the beams took place with crushing of the



Fig. 7 Crack pattern and failure mode of the reinforced GPC specimen

concrete in the compression zone along with the buckling of the compressive steel bars and hanger bars. The crack pattern and the failure mode of the beam are shown in Fig. 7.

7.4 Moment carrying capacity

The ultimate moment carrying capacities (MCC) of the beams were theoretically calculated conforming to IS 456-2000 and were compared with those of the experimental results. The experimental and theoretical results are shown in Table 7. The moment-curvature relationship is shown in Figs. 8 and 9. The Table 7 shows that the observed tested

Table 8 Material properties of GPCs for ANSYS 13.0

Material property	FA-GPC under			FA PSA-GPC under		
	OC	EEC	AC	OC	EEC	AC
Young's modulus (E), $\times 10^5$ N/mm ²	0.29	0.234	0.22	0.25	0.25	0.24
Poisson's ratio	0.15	0.135	0.13	0.147	0.145	0.14
Density, kg/m ³	2447	2345	2100	2431	2401	2378

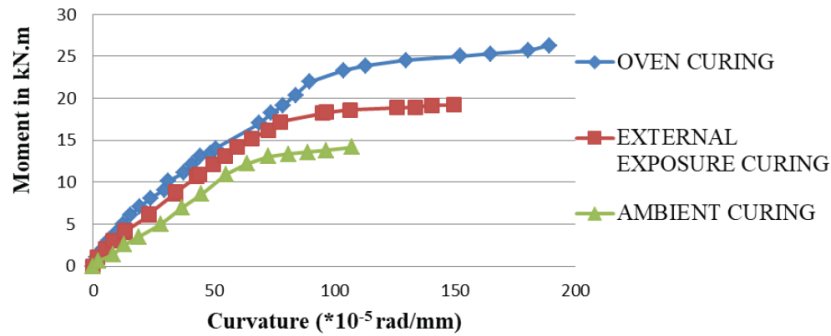


Fig. 8 Load moment-curvature relationship for FA-GPC beams

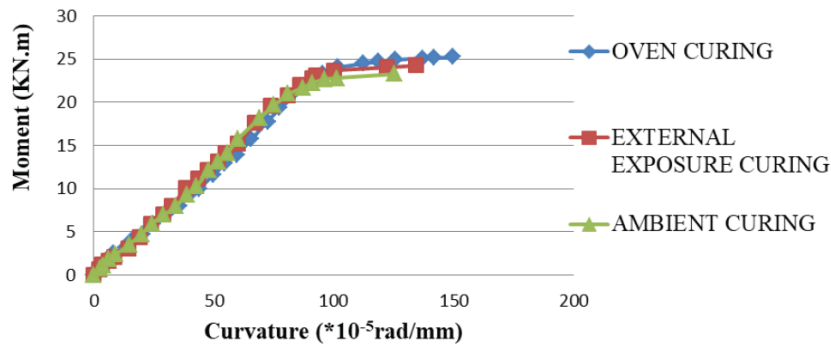


Fig. 9 Load moment-curvature relationship for FA-PSA GPC beams

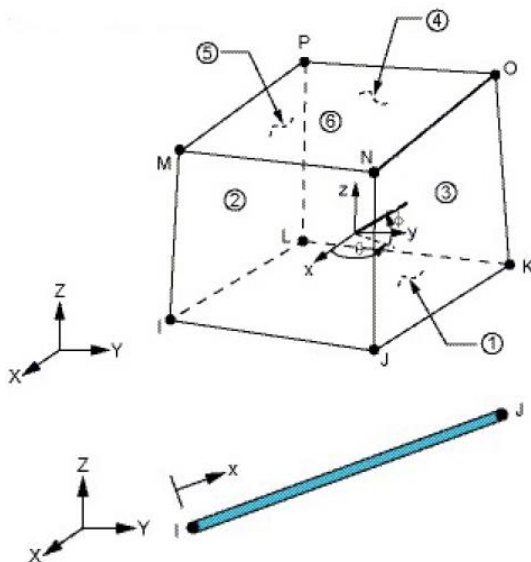


Fig 10 Solid 65 and Link 8 geometry

flexural capacity of the FA-GPC OC beams is higher than the predicted ultimate MCC values. For FA-GPC EEC and FA-GPC AC beams, the observed flexural strengths are lower than the predicted strength.

Whereas in the case of FA-PSA GPC beams, the tested flexural capacity was higher than that of their predicted values under all the three curing conditions. The similar behaviour in LCC and moment capacity was observed under ambient conditions by using FA and GGBS as the source materials in the reinforced GPC beams in the experiment conducted by Dattatreya *et al.* (2011).

8. Finite element modelling

The experimental results of the FA-GPC and FA-PSA GPC beams were numerically validated by ANSYS.

Element type used for analysis was Solid 65 for concrete and Link 8 for steel bars and stirrups (Fig. 10). In Solid65 elements, each element is defined by eight nodes. Each node has three degrees of freedom (translations in the nodal x , y and z directions). Link 8 is a uniaxial tension-compression element with three degrees of freedom at each node (translations in the nodal x , y and z directions). Input data for ANSYS such as material properties of concrete and steel are shown in Tables 8 and 9. The shear transfer coefficient β , which shows the conditions of crack face, normally ranges between 0 and 1.0. A value of 0.9 was adopted in this study for open shear coefficient and 0.5 for

Table 9 Material properties of steel for ANSYS 13.0

Material property	ϕ12 mm	ϕ10 mm	ϕ8 mm
Young's modulus (<i>E</i>), GPa	206	223	221
Yield strength, N/mm ²	560	550	595
Poisson's ratio	0.278	0.284	0.25

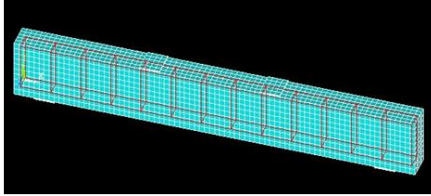


Fig 11 Finite element model of beam in ANSYS

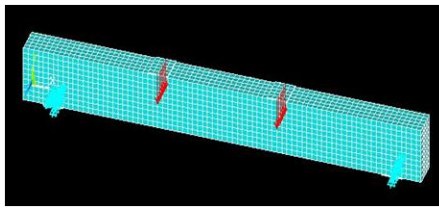


Fig. 12 Loads and supports of beam

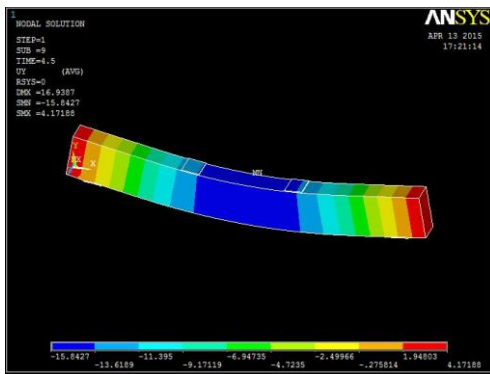


Fig. 13 Typical deflected shape of GPC beam in ANSYS

the closed shear coefficient.

As same nodes are used for concrete and reinforcement, hence it is assumed that there is a perfect bond between these two materials (Kachlakev *et al.* 2001, Fanning 2001, Santhakumaret *al.* 2007). The stress strain curves measured from the experiments were used for analysis. Figs. 11 and 12 show the model of the beam and loading pattern of the beam in ANSYS 13.0.

9. Comparison of experimental and numerical results of FA-GPC and FA-PSA GPC beams

9.1 Load-deflection characteristics

The load deflection curves predicted using ANSYS were compared with those obtained from experimental results. Fig. 13 shows a typical deflected shape of the GPC beam in ANSYS. The ultimate loads and midspan deflections from experimental ($P_U)_E$ and $(\delta_U)_E$ and analytical $(P_U)_A$ and $(\delta_U)_A$ results are shown in Table 10. From Figs. 14(a)-(c) and

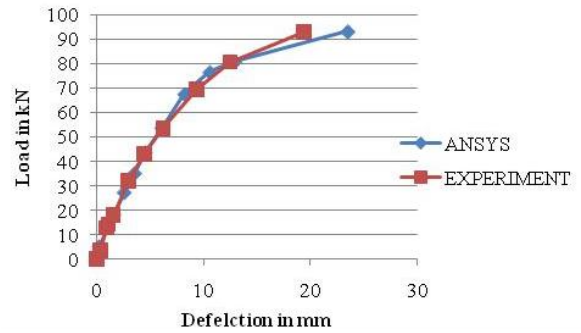


Fig. 14(a) Experimental vs. FEM load deflection response of FA-GPC OC beams

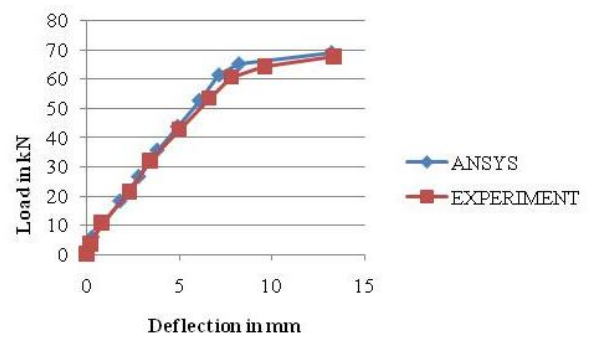


Fig. 14(b) Experimental vs. FEM load deflection response of FA-GPC EEC beams

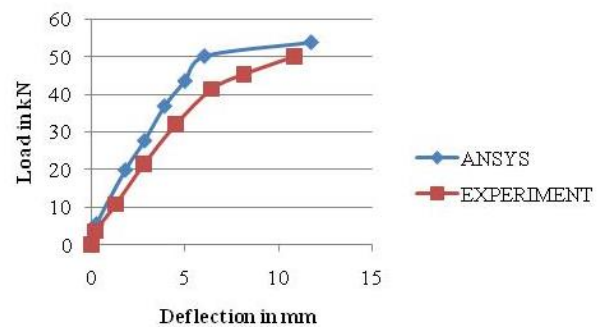


Fig. 14 (c) Experimental vs. FEM load deflection response of FA-GPC AC beams

15(a)-(c), it is clear that in general the load deflection plots for the GPC beams from finite element analysis agree well with the experimental data. But there is a slight difference in the finite element load deflection curve with the experimental curve. This small deviation may be caused due to several effects such as the assumption that made in the FEA that a perfect bond exists between the concrete and steel reinforcement, which in reality would not be possible as slip of the reinforcement may occur. FEA model of a reinforced concrete beam in general predicts that the beam is stiffer than it actually is, because the materials in the FE model are perfectly homogenous, unlike those in the actual structure. Moreover, the boundary conditions strictly defined in the FE model are more rigid than the actual structure. Additionally, micro-cracks in the concrete as well as other imperfections in construction may lessen the stiffness of the actual beam.

Table 10 Comparison of ultimate loads and deflections obtained from experimental and analytical studies

Beam ID	Ultimate load (kN)			Mid span deflection(mm)		
	Experimental (P_{UE})	Analytical (P_{UA})	Ratio (P_{UA}/P_{UE})	Experimental (δ_{UE})	Analytical (δ_{UA})	Ratio (δ_{UA}/δ_{UE})
FA-GPC OC	92.82	93.176	1.004	19.34	20.815	1.076
FA-GPC EEC	67.3	68.8	1.022	13.32	14.434	1.084
FA-GPC AC	49.98	53.89	1.078	10.84	11.789	1.088
FA-PSA GPC OC	89.25	90.89	1.018	15.2	16.958	1.116
FA-PSA GPC EEC	85.68	87.6	1.022	14.2	15.809	1.113
FA-PSA GPC AC	82.11	83.4	1.016	13.32	15.405	1.157

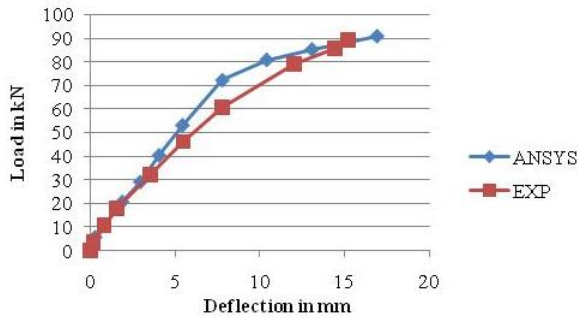


Fig. 15(a) Experimental vs. FEM load deflection response of FA-PSA GPC OC beams

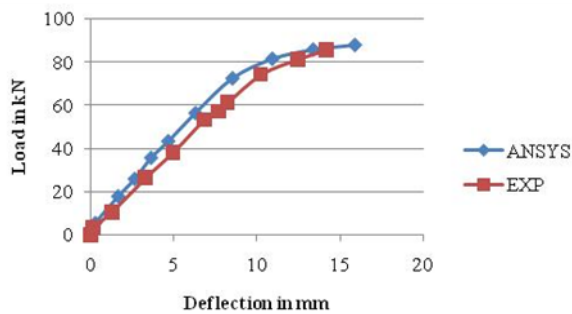


Fig. 15(b) Experimental vs FEM load deflection response of FA-PSA GPC EEC beams

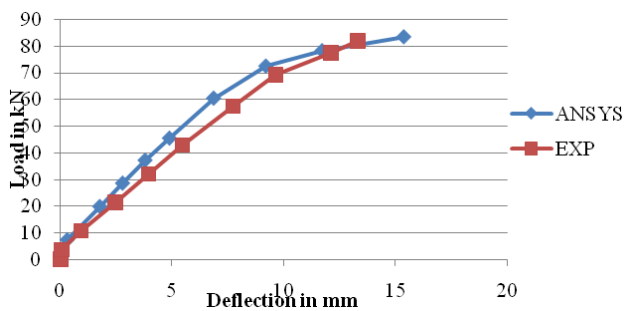


Fig. 15(c) Experimental vs FEM load deflection response of FA-PSA GPC AC beams

9.2 Crack pattern and failure mode

A comparison of the crack patterns from the numerical findings with the crack patterns from experimental test is shown in Fig. 16(a)-(f). Crack patterns obtained from the finite element analysis at the last converged load steps and the failure photographs from the tested beam are similar.

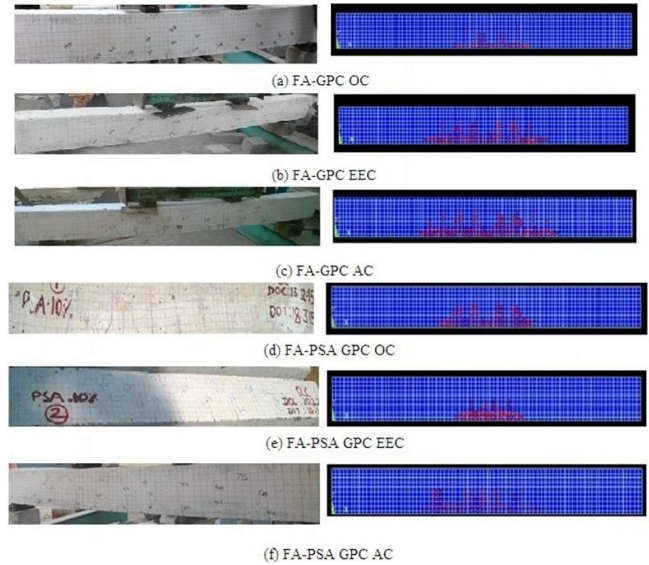


Fig. 16 Crack pattern of experimental and ANSYS modelled beams

Flexural cracks occurred in the midspan and were followed by diagonal shear cracks near the support. The failure modes of the FEA models show good agreement with those obtained from experiments.

10. Conclusions

1. The load deflection characteristics obtained for the FA-GPC beams and FA-PSA-based GPC beams from experimental testing were having almost similar curvature.
2. The crack patterns observed and the modes of failure for FA-PSA GPC beams were found to be similar to those of the FA-GPC beams. The beams failed initially by yielding of the tensile reinforcement followed by the crushing of concrete in the compressive face.
3. The FA-GPC OC beams show increase in FCL values to about 37.5% and 75% compared to FCL of FA-GPC beams under EEC and AC conditions, respectively. There is an improvement in both LCC and MCC by about 26.95% and 46.15% under FA-GPC OC when compared to those of the FA-GPC beams under EEC and AC conditions, respectively, due to increase in the rate of geopolymerization because of higher temperature.

4. The inclusion of PSA into the GPC for the replacement of FA for about 10% increases the FCL by about 16.67% and 66.67% under EEC and AC conditions respectively. The inclusion of PSA also improves the both average LCC and MCC by about 20.866% and 39.13% under EEC and AC conditions, respectively, compare to FA-GPC under the same curing conditions. It is because of its chemical composition (CaO) that improves the geopolymerization reaction under the low-temperature curing.
5. The finite element model was slightly stiffer than the actual beam.
6. The measured deflection of beam and the predicted deflection using ANSYS agree quite well.
7. Flexural behaviour of FA-GPC and FA-PSA GPC beams was almost similar but there were some differences between both the beam depending on the inclusion of PSA and the curing conditions of the concrete.
8. The GPC containing PSA was found to perform adequately as a structural component and could be considered as a potential candidate material for replacing FA in GPC.
9. GPC can be developed for structural application from low-calcium fly ash and PSA under all the three curing condition viz., OC, EEC, and AC.

References

- Ambily, P.S., Madheswaran, C.K., Sharmila, S. and Muthiah, S. (2011), "Experimental and analytical investigations on shear behaviour of reinforced geopolymer concrete beams", *Int. J. Civil Struct. Eng.*, **2**(2), 673.
- Anuradha, R., Sreevidya, V. and Venkatasubramani, R. (2012), "Geopolymer reinforced concrete beams made with and without sand", *J. Struct. Eng.*, **39**(2), 254-262.
- Battaglia, A., Calace, N., Nardi, E., Petronio, B.M. and Pietroletti, M. (2003), "Paper mill sludge-soil mixture: kinetic and thermodynamic tests of cadmium and lead sorption capability", *Microchem. J.*, **75**(2), 97-102.
- BIS 383 (1970), *Specifications for Coarse and Fine Aggregates from Natural Sources for Concrete*, Bureau of Indian Standards, New Delhi, India.
- Dattatreya, J.K., Rajamane, N.P., Sabitha, D., Ambily, P.S. and Nataraja, M.C. (2011), "Flexural behaviour of reinforced geopolymer concrete beams", *Int. J. Civil Struct. Eng.*, **2**(1), 138-159.
- Davidovits, J. (1994), "Global warming impact on the cement and aggregates industries", *World Res. Rev.*, **6**(2), 263-278.
- Davidovits, J. (2005), "The polysialate terminology: a very useful and simple model for the promotion and understanding of green-chemistry", *Geopolymer, Green Chemistry and Sustainable Development Solutions: Proceedings of the World Congress Geopolymer*, Geopolymer Institute, Saint-Quentin, France, July.
- Fanning, P. (2001), "Nonlinear models of reinforced and post-tensioned concrete beams", *Electron. J. Struct. Eng.*, **2**(1), 122-132.
- Fernandez-Jimenez, A., García-Lodeiro, I. and Palomo, A. (2015), "Development of new cementitious materials by alkaline activating industrial by-products", *Second International Conference on Innovative Materials, Structures and Technologies*, IOP Conference Series: Materials Science and Engineering, Riga, Latvia, October.
- Geng, X., Deng, J. and Zhang, S.Y. (2006), "Effects of hot pressing parameters and wax content on the properties of binderless fiberboard made from paper mill sludge", *J. Wood Fiber Sci.*, **38**(4), 736-741.
- Hardjito, D. and Rangan, B.V. (2005), "Development and properties of low-calcium fly ash-based geopolymer concrete", Research Report GC1; Faculty of Engineering, Curtin University of Technology, Perth, Australia.
- Hardjito, D., Wallah, S., Sumajouw, D. and Rangan, B. (2004), "Properties of geopolymer concrete with fly ash as source material: effect of mixture composition", *The 7th CANMET/ACI International Conference on Recent Advance in Concrete Technology*, Las Vegas, USA, May.
- IS 10262 (2009), Guidelines for Concrete Mix Design Proportioning, Bureau of Indian Standards, New Delhi, India.
- IS 456 (2000), Plain and Reinforced Concrete-Code of Practice, Bureau of Indian Standards, New Delhi, India.
- IS: 516 (1959) *Methods of Tests for Strength of Concrete*, Bureau of Indian Standards, New Delhi, India.
- Jindal, B., Singhal, D., Sharma, S.K., Ashish, D. and Parveen, K. (2017), "Improving compressive strength of low calcium fly ash geopolymer concrete with alccofine", *Adv. Concrete Constr.*, **5**(1), 17-29.
- Kachlakev, D., Miller, T., Yim, S., Chansawat, K. and Potisuk, T. (2001), "Finite element modeling of reinforced concrete structures strengthened with FRP laminates", Report for Oregon Department of Transportation, Salem, USA, May.
- Kannapiran, K., Sujatha, T. and Nagan, S. (2013), "Comparative study on the flexural behaviour of reinforced cement concrete and reinforced geopolymer concrete beams", *J. Struct. Eng.*, **39**(5), 598-604.
- Khale, D. and Chaudhary, R. (2007), "Mechanism of geopolymerization and factors influencing its development: a review", *J. Mater. Sci.*, **42**, 729-746.
- Madheswaran, C.K., Ambily, P.S., Lakshmanan, N., Dattatreya, J.K. and Sathik, J.K. (2014), "Shear behavior of reinforced geopolymer concrete thin-webbed T-beams", *ACI Mater. J.*, **111**(1), 89-98.
- Manjunath, G.S., Radhakrishna, C. and Giridhar, M.J. (2011), "Compressive strength development in ambient cured geopolymer mortar", *Int. J. Earthq. Sci. Eng.*, **4**(10), 830-834.
- Mun, S.P. and Ahn, B.J. (2001), "Chemical conversion of paper sludge incineration ash into synthetic zeolite", *J. Ind. Eng. Chem.*, **7**(5), 292-298.
- Nguyen, K.T., Namshik, A., Le, T.A. and Lee, K. (2016), "Theoretical and experimental study on mechanical properties and flexural strength of fly ash-geopolymer concrete", *Constr. Build. Mater.*, **106**(3), 65-77.
- Parveen, S.D. (2017), "Development of mix design method for geopolymer concrete", *Adv. Concrete Constr.*, **5**(4), 377-390.
- Pires, E.F.C., Silva, F.J., Pereira, R.A. and Darwish, F.A.I. (2014), "Fracture toughness of geopolymer concrete for precasting RC beams", *15th NOCMAT 2014*, Pirassununga SP, Brazil BioSMat., November.
- Puertas, F., Martinez-Ramirez, S., Alonso, S. and Vazquez, T. (2000), "Alkali-activated fly ash/slag cement strength behaviour and hydration products", *Cement Concrete Res.*, **30**(10), 1625-1632.
- Ridzuan, A.R.M., Khairulniza, A.A. and Fadhil, M.A. (2013), "The evaluation of high calcium green polymeric concrete", *Adv. Mater. Res.*, **626**(4), 776-780.
- Santhakumar, R., Dhanaraj, R. and Chandrasekaran, E. (2007), "Behaviour of retrofitted reinforced concrete beams under combined bending and torsion: A numerical study", *Electron. J. Struct. Eng.*, **7**(7), 34-45.
- Shi, C., Krivenko, P.V. and Roy, D. (2006) *Alkali-Activated*

- Cements and Concrete*, Taylor and Francis, Oxford, London, New York.
- Silverstrim, T., Martin, J. and Rostami, H. (1999), "Geopolymeric fly ash cement", *Proceeding of Geopolymere'99*, Saint-Quentine, France, June.
- Silverstrim, T., Rostami, H., Clark, B. and Martin, J. (1997), "Microstructure and properties of chemically activated fly ash concrete", *Proceedings of the 19th International Conference on Cement Microscopy*, International Cement Microscopy Association, Cincinnati, OH, Washington, April.
- Temuujin, J., Williams, R.P. and Riessen, A. (2009), "Effect of mechanical activation of fly ash on the properties of geopolymer cured at ambient temperature", *J. Mater. Proc. Technol.*, **209**(12), 5276-5280.
- Wallah, S.E. and Rangan, B.V. (2006), "Low-calcium fly ash-based geopolymer concrete: long-term properties", Research Report GC 2, Curtin University of Technology, Perth, Australia.